J. Am. Chem. Soc. 1986, 108, 5434-5440

Reversible Oxidation and Rereduction of Magnesium Phthalocyanine Electrodes. Electrochemical Behavior and in Situ Raman Spectroscopy

J. L. Kahl,[†] Larry R. Faulkner,*[†] K. Dwarakanath,[‡] and H. Tachikawa*[‡]

Contribution from the Department of Chemistry and Materials Research Laboratory, University of Illinois, Urbana, Illinois 61801, and Department of Chemistry, Jackson State University, Jackson, Mississippi 39217.

Received July 11, 1985.
Revised Manuscript Received June 2, 1986

Abstract: Reversible oxidation and rereduction of magnesium phthalocyanine (MgPc) thin films (1000–2000 Å thick) on gold electrodes have been observed in the potential range from 0.0 to 0.9 V vs. SCE in various electrolytes, including aqueous NaCl, $NaNO_3$, $NaClO_4$, and potassium hydrogen phthalate (KHP). In situ Raman spectra recorded during oxidation and rereduction show spectral changes in the 400–1800-cm^{-1} range that can be related to the vibrational modes of ring structures in MgPc, hence the oxidation seems to occur in the ligand. The spectroscopic results unambiguously demonstrate the movement of anions into and out of the electrode during oxidation and rereduction processes. Both cyclic voltammetry and chronocoulometry showed that smaller anions allow full oxidation at rapid rates, whereas larger ones inhibit the oxidation, at least with respect to rate. Auger electron spectrometry showed that anions appear to be homogeneously distributed in partially oxidized films.

The electrochemical properties of thin films of phthalocyanines coated onto conducting substrates have raised a good deal of interest. The ability of some phthalocyanines to catalyze the electroreduction of molecular oxygen has stimulated much of the activity,[1] but there has also been a sizable body of research devoted to the behavior of phthalocyanine thin films as semiconducting electrodes.[2] Related to both of these domains but attractive in its own right, is the ability of many thin films of phthalocyanines to undergo stoichiometric oxidation and reduction, sometimes reversibly, with changes in the color of the film and with uptake and expulsion of charge-compensating ions. The electrochromism might have applications in display technology,[3] and the capability for charge storage could be useful in new kinds of batteries,[4] but the redox transformations are worthy of study from a fundamental standpoint, because they allow one to examine ion- and electron-transport in compact layers on electrodes, which is a general topic of currency. Moreover, the onsets of the electrochromic oxidations and reductions define the domains of potential where semiconducting behavior might be found, and these processes could affect the true identities of electrocatalysts in phthalocyanine systems studied for their catalytic properties.

The most extensive work on electrochromism has been done by Nicholson and co-workers,[3,5] who have stressed the dual-ring complex lutetium diphthalocyanine as an active material. Several other groups have also reported results for rare-earth diphthalocyanines.[6] In 1979, Kahl and Faulkner[7] made an oral report of their discovery that single-ring phthalocyanines could also show this effect, and they suggested that the effect arose from stoichiometric oxidation and rereduction of the film. Shortly thereafter, Gavrilov et al.[6c] described similar oxidation and rereduction processes for tetra-*tert*-butyl derivatives of cobalt and zinc phthalocyanines that had been "rubbed" onto In_2O_3-coated glass. Green and Faulkner[8] followed up Kahl's early work in a more quantitative manner and extended his discovery to a greater variety of systems. They showed conclusively that the oxidative conversions involved one or two electrons per phthalocyanine molecule, depending on the metal center's ability to undergo oxidation. Zinc phthalocyanine was the most carefully examined system. Green and Faulkner suggested that its one-electron oxidation and rereduction very likely takes place in the phthalocyanine ring of ZnPc, since the Zn center is not expected to offer any electroactivity. Anions from supporting electrolytes were shown to penetrate into the film and balance the charge during the oxidation. It was also reported that the sizes of the anions affected their ability to enter the films and consequently affected the rate and degree of oxidation.

This article describes the early work of Kahl and Faulkner on magnesium phthalocyanine (MgPc), which has not been discussed

---

[†] University of Illinois.

[‡] Jackson State University.

(1) This area has a large literature that cannot be reviewed fully here. Much of it deals with homogeneous electrocatalysis or electrocatalysis by adsorbed layers, rather than compact films. A few original and very recent references are the following: (a) Jasinski, R. *Nature* (*London*) **1964**, *201*, 1212. (b) Meier, H.; Albrecht, W.; Tschirwitz, V.; Zimmerhackl, E. *Ber. Chem.* **1973**, *77*, 843. (c) Appleby, A. J.; Savy, M. In *Electrode Materials and Processes for Energy Conversion and Storage*: McIntyre, J. D. E., Srinivasan, S., Will, F. G., Eds.; The Electrochemical Society Softbound Proceedings Series: Princeton, NJ, 1977; p 321. (d) Appleby, A. J.; Fleisch, J; Savy, M. *J. Catal.* **1976**, *44*, 281. (e) Zagal, J.; Sen, R. K.; Yeager, E. *J. Electroanal. Chem. Interfacial Electrochem.* **1977**, *83*, 207. (f) Melendres, C. A.; Feng, X. *J. Electrochem. Soc.* **1983**, *130*, 811. (g) Van Den Brink, F.; Visscher, W.; Barendrecht, E. *J. Electroanal. Chem.* **1983**, *157*, 283, 305. (h) Paliteiro, C.; Hamnett, A.; Goodenough, J. B. *J. Elecroanal. Chem.* **1984**, *160*, 359.

(2) This area has a truly massive literature, especially as it relates to electrophotography. With a view restricted to a more conventional electrochemical context, the following references are relevant: (a) Tachikawa, H.; Faulkner, L. R. *J. Am. Chem. Soc.* **1978**, *100*, 4379. (b) Fan, F. R.; Faulkner, L. R. *J. Am. Chem. Soc.* **1979**, *101*, 4779. (c) Faulkner, L. R.; Tachikawa, H.; Fan, F.-R.; Fischer, S. G. *Adv. Chem. Ser.* **1980**, *184*, 113. (d) Armstrong, N. R.; Shepard, V. R., Jr. *J. Electroanal. Chem. Interfacial Electrochem.* **1982**, *131*, 113. (e) Leempoel, P.; Fan, F.-R.; Bard, A. J. *J. Phys. Chem.* **1983**, *87*, 2048. (f) Linkous, C.; Klofta, T.; Armstrong, N. R. *J. Electrochem. Soc.* **1983**, *130*, 1050.

(3) Nicholson, M. M.; Weismuller, T. P. "A Study of Colors in Lutetium Diphthalocyanine Electrochromic Displays"; report from Autonetics Strategic Systems Division, C82-268/201 (NTIS Order No. AD-A120483), Rockwell International, Anaheim, CA, 1982.

(4) (a) Yamaki, J.; Yamaji, A. *J. Electrochem. Soc.* **1982**, *129*, 5. (b) Dalard, F.; Deroo, D.; Djellab, H.; Cohen, J. P.; Addad, Mercier, J. *J. Power Sources* **1985**, *14*, 71.

(5) (a) Nicholson, M. M.; Pizzarello, F. A. *J. Electrochem. Soc.* **1979**, *126*, 1490. (b) Nicholson, M. M.; Pizzarello, F. A. *J. Electrochem. Soc.* **1980**, *127*, 821. (c) Pizzarello, F. A.; Nicholson, M. M. *J. Electron Mater.* **1980**, *9*, 231. (d) Nicholson, M. M.; Pizzarello, F. A. *J. Electrochem. Soc.* **1980**, *127*, 2617. (e) Nicholson, M. M.; Pizzarello, F. A. *J. Electrochem. Soc.* **1981**, *128*, 1288. (f) Nicholson, M. M.; Pizzarello, F. A. *J. Electrochem. Soc.* **1981**, *128*, 1741. (g) Nicholson, M. M.; Weismuller, T. P.; Pizzarello, F. A. "Mechanisms and Kinetics of Diphthalocyanine Electrode Processes"; report from Autonetics Strategic Systems Division, C83-22/201, AOSR-TR-83-0721 (NTIS Order No. AD-A131726), Rockwell International, Anaheim, CA, 1983.

(6) (a) Moskalev, P. N.; Kirin, I. S. *Russ. J. Phys. Chem.* (*Engl. Transl.*) **1972**, *46*, 1019. (b) Yamana, M. *Oyo Butsuri* **1979**, *48*, 441. (c) Gavrilov, V. I.; Butasova, N. V.; Luk'yanets, E. A.; Shelepin, I. V. *Electrokhimiya* **1980**, *16*, 1611. (d) Walton, D.; Ely, B.; Elliott, G. *J. Electrochem. Soc.* **1981**, *128*, 2479 (e) Tomilova, L. G.; Chernykh, E. V.; Gavrilov, V. I.; Shelepin, I. V.; Derkacheva, V. M.; Luk'yanets, E. A. *Zh. Obshch. Khim.* **1982**, *52*, 2606. (f) Tomilova, L. G.; Chernykh, E. V.; Ioffe, N. T.; Luk'yanets, E. A. *Zh. Obshch. Khim.* **1983**, *53*, 2594.

(7) Faulkner, L. R.; Kahl, J. L. Presented at the 11th Central Regional Meeting of the American Chemical Society, Columbus, OH, May 7–9, 1979.

(8) Green, J. M.; Faulkner, L. R. *J. Am. Chem. Soc.* **1983**, *105*, 2950.

0002-7863/86/1508-5434$01.50/0

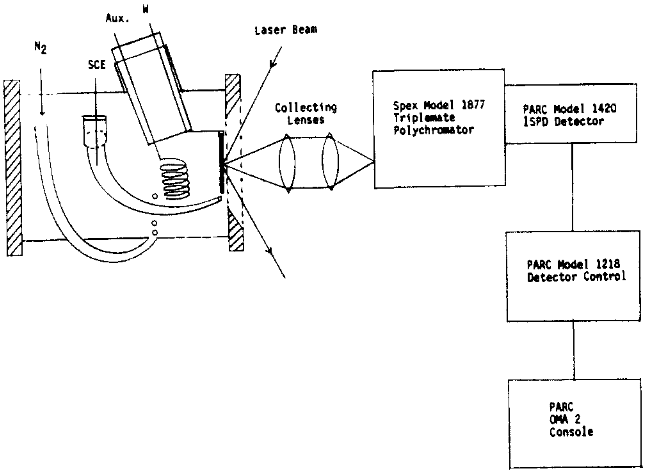

Figure 1. Experimental setup for in situ Raman spectroscopy of thin film MgPc electrodes. The working electrode contact is denoted by "W".

in the printed literature. To that material, we are adding here a report on the Raman spectroscopy of the same system, which has just been carried out by Dwarakanath and Tachikawa.

There have been numerous reports of Raman spectroscopic investigations of metal phthalocyanines, both in thin films[9] and as adsorbed species on electrode surfaces.[10] The reported Raman spectroscopic studies of phthalocyanines in electrochemical situations have mainly involved adsorbed layers and have addressed questions of concern in electrocatalysis. To our knowledge, there has been no report of in situ Raman spectroscopy of phthalocyanine thin films during electrochromic oxidations and rereductions. This paper describes such experiments.

Experimental Section

Magnesium phthalocyanine (Eastman Kodak) was sublimed twice in vacuo before use. MgPc thin films (1000–2000 Å thick) were vapor deposited by using either a Varian Model 3118 (Jackson State) or a Varian Model 3117 (Illinois) vacuum bell jar system. Films were deposited onto glass slides (2.5 cm × 2.5 cm, 1.6 mm thick) previously coated through a mask with 70 Å of Cr and then with 500 Å of Au. Depositions were performed at 5×10^{-7} torr and at rates of 1–10 Å/s. The pattern used for the Au and Cr layers was similar to that used earlier.[2a,b] In most of the work, a magnesium fluoride thin film (1500 Å) was deposited over part of the gold pattern before deposition of the phthalocyanine in order to define a disk-shaped working electrode having a geometric area of about 0.2 cm^2. When the MgF_2 was not deposited, the glass slide was only immersed to the extent needed to cover this disk with electrolyte.

All electrolytes were reagent grade and were used without further purification. Aqueous solutions were made with deionized, doubly distilled water.

In Raman scattering experiments, the thin film electrode was approximately 1 mm from the window of an electrochemical cell. Figure 1 shows the experimental setup. A platinum helix was used as an auxiliary electrode. The reported potentials were measured with respect to a saturated calomel electrode (SCE). The salt bridge for the SCE reference electrode was filled with the working electrolyte to minimize contamination of the main solution.

Electrochemical measurements were made with an EG&G Princeton Applied Research Corp. (PARC) Model 173 potentiostat, a PARC Model 179 digital coulometer, a PARC Model 175 signal generator, and a Houston Instrument Model 2000 x-y recorder, or with a Bioanalytical Systems BAS-100 cybernetic potentiostat.

Table I. Chronocoulometric Responses to a Continuous Square Wave[a]

cycle	oxidation[b]	reduction[b]
	1 M KCl	
1st	7.2×10^{-9}	7.0×10^{-9}
2nd	6.8×10^{-9}	6.1×10^{-9}
100th	3.0×10^{-9}	2.9×10^{-9}
	1 M $NaClO_4$	
1st	7.1×10^{-9}	6.8×10^{-9}
2nd	4.1×10^{-9}	3.7×10^{-9}
100th	2.7×10^{-9}	2.8×10^{-9}
	0.5 M KHP	
1st	0.13×10^{-9}	0.13×10^{-9}
2nd	0.74×10^{-9}	0.72×10^{-9}
100th	3.0×10^{-9}	3.1×10^{-9}

[a] Pulse width = 10 s. There are 7.3×10^{-9} mol of MgPc in each 2000-Å film and 2.2×10^{-11} mol on the surface of a flat substrate. Film thickness was monitored with a Sloan DTM 200 quartz microbalance. Density was taken as 1.5; see ref 8. [b] Mol of electrons passed.

All electrolyte solutions except KHP were adjusted to pH 6.0 ± 0.1 with HCl, HNO_3, or NaOH. These solutions were deaerated by bubbling with prepurified N_2 gas. A nitrogen atmosphere was maintained in the cell during electrochemical and Raman measurements.

In Raman work, the excitation beam was brought in at a 60° angle from the horizontal. Raman measurements were made by a system consisting of a homemade sample stand with optics,[11] a Spex Model 1877 Triplemate polychromator, and an EG&G PARC Model 1420 ISPD detector with an EG&G PARC Model 1218 controller and OMA II console system. A Coherent Radiation Model CR-2 Ar^+ laser was used as an excitation source. The slit widths of the spectrometer were set at 150 μm, and a 1200 groove–mm grating was used. Spectral resolution was about 1.4 cm^{-1}. The spectrometer was calibrated by using a spectrum from a ZnPc thin film (1000 Å) electrode that had been previously examined on a calibrated Spex Model Ramalog 5 Raman spectrophotometer. The accuracy of frequency measurements is estimated to be ±5 cm^{-1}. In situ Raman spectra were collected in approximately 30 s while the potential of the working electrode was controlled by a PARC Model 173 potentiostat.

Auger electron spectrometry was performed with a Physical Electronics Model 545 scanning Auger microprobe. Typical conditions involved a primary electron beam of 4-KeV energy and 2.5-μA current rastered over a 0.1-mm square area. Depth profiles were obtained by repetitively scanning over appropriate Auger transitions during simultaneous sputtering of the sample by a 1-KeV, 2-mA argon ion beam.

Results and Discussion

Electrochemistry. Cyclic voltammetric curves of the MgPc electrode in both 1.0 M $NaNO_3$ and 0.4 M KHP solutions are shown in Figure 2a and b, respectively. The oxidation peak in the first cycle (E_{pa}) in 1.0 M $NaNO_3$ showed a significant overpotential, and its peak potential was found to be dependent on the scan rate (E_{pa} = 0.75, 0.65, and 0.59 V at scan rates of 100, 50, and 10 mV/s, respectively). The anodic and cathodic peak currents gradually decreased in successive cycles and reached a steady state after about 50 cycles. In contrast to the behavior in nitrate solution, there was no discernable oxidation peak in the first cycle in 0.4 M KHP when the potential was scanned to 0.9 V vs. SCE. However, there was a cathodic peak current in the first negative sweep. In the second positive sweep, there was a matching oxidation peak. Subsequently, the anodic and cathodic peak currents both increased steadily and reached a steady state after about 20 cycles. The steady-state peak currents in 0.4 M KHP solution were almost identical with those observed in 1.0 M $NaNO_3$. However, the anodic peak potential at steady state in 0.4 M KHP was 0.45 V vs. SCE, compared with 0.60 V vs. SCE in $NaNO_3$ solution. The separation between the anodic and cathodic peaks (ΔE_p) in KHP was smaller (70 mV) than in $NaNO_3$ (150 mV).

Multicyclic chronocoulometric responses were recorded for MgPc electrodes in 1.0 M KCl, 1.0 M $NaClO_4$, and 0.5 M KHP solutions. Each cycle consisted of a potential step from 0.0 to 0.9

---

(9) (a) Aroca, R.; Dilella, D. P.; Loutfy, R. O. *J. Phys. Chem. Solids* **1982**, *43*, 707. (b) Melendres, C. A.; Cafasso, F. A. *J. Electrochem. Soc.* **1981**, *128*, 755. (c) Jennings, C.; Aroca, R.; Hor, A. M.; Loutfy, R. O. *J. Raman Spectrosc.* **1984**, *15*, 34. (d) Hayashi, S.; Samejima, M. *Surface Sci.* **1984**, *137*, 442.

(10) (a) Melendres, C. A. *J. Phys. Chem.* **1980**, *84*, 1936. (b) Kotz, R.; Yeager, E. *J. Electroanal. Chem.* **1980**, *113*, 113. (c) Simic-Glavaski, B.; Zecevic, S.; Yeager, E. *J. Electroanal. Chem.* **1983**, *150*, 469. (d) Melendres, C. A.; Rios, C. B.; Feng, X.; McMasters, R. *J. Phys. Chem.* **1983**, *87*, 3529. (e) Zecevic, S.; Simic-Glavaski, B.; Yeager, E.; Lever, A. B. P.; Minor, P. C. *J. Electroanal. Chem.*, in press.

(11) Fairchild, C.; Tachikawa, H. in preparation.

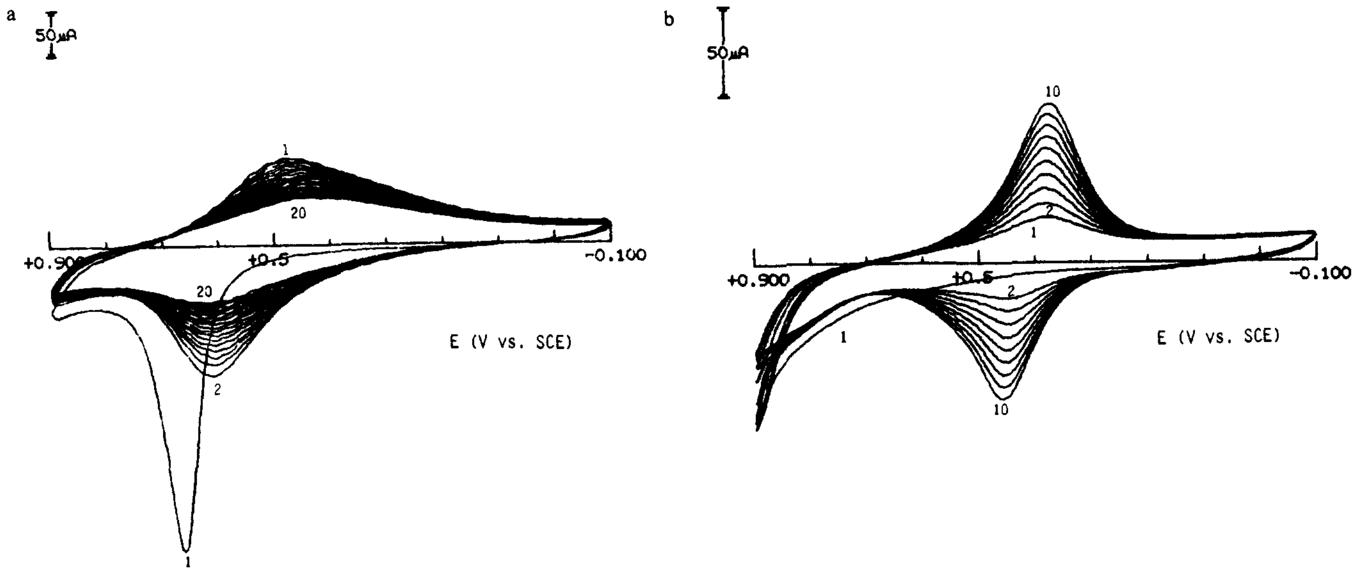

Figure 2. Cyclic voltammograms at a MgPc thin film electrode (1000 Å) in (a) 1.0 M $NaNO_3$ and (b) 0.4 M KHP. All scans start at 0 V and first move positively at 50 mV/s.

V and the return to 0.0 V. The data in Table I suggest that there is complete oxidation of the MgPc film in the first step in both Cl^- and ClO_4^-, whereas HP^- allows only a "surface" oxidation. These results suggest that the oxidation of the MgPc film is controlled by the transport of charge-compensating anions (An^-)

$$MgPc + An^- \rightarrow MgPc^+ \cdot An^- + e^- \qquad (1)$$

Nitrate, being small,[8] seems to move quickly through the film and allows oxidation to occur in a narrow potential range as shown in Figure 2a. Biphthalate (HP^-), much larger, apparently cannot move readily throughout the film; therefore, only a limited oxidation can take place. Dianions, such as SO_4^{2-}, HPO_4^{2-}, and SiF_6^{2-}, permitted no oxidation of the MgPc electrode at potentials up to +0.9 V.

No dependence on cation transport for the rereduction was observed. Cyclic voltammograms in LiCl, NaCl, RbCl, CsCl, $MgCl_2$, and tetraethylammonium chloride were virtually identical. This behavior suggests a rereduction step that requires anion transport out of the film

$$MgPc^+ \cdot An^- + e^- \rightarrow MgPc + An^- \qquad (2)$$

The chronoamperometric data shown in Figure 3 demonstrate that the kinetics of oxidation and rereduction depend on the anion involved. Complete oxidation of the MgPc film with compensation by Cl^- takes less than 0.2 s, but with ClO_4^- it takes 0.7 s. With HP^- it takes only 0.1 s for the less extensive conversion seen in that case. In the presence of Cl^- and ClO_4^-, the rereductions are much slower than the oxidations. One can see in Figure 3a that with Cl^-, only a third of the reduction occurs between 1.0 and 1.2 s, while the remaining two thirds takes place in the tail of the current decay. Complete rereduction of the film in Cl^- and ClO_4^- solutions, as represented in Figure 3a and b and Table I, takes up to 10 s for the first cycle. This slow rate of rereduction could be the result of slow charge-transfer kinetics, an alteration of the crystalline structure, or a much lower conductivity in the oxidized film, compared to the reduced one. Plots of i vs. t and $t^{1/2}$ for the first cycle are nonlinear.

The rereduction of the film in KHP (Figure 3), apparently being only a reaction of limited extent, as the oxidation was, occurs in 0.1 s. By the 100th cycle (Table I), all three anions show a charge-transfer capacity corresponding to 25–30% of that of the original film. This phenomenon was reported for other metal phthalocyanines, and loss in charge capacity for small anions was attributed to an electrical isolation of domains in this film on a grain-by-grain basis after many oxidation and rereduction cycles.[8]

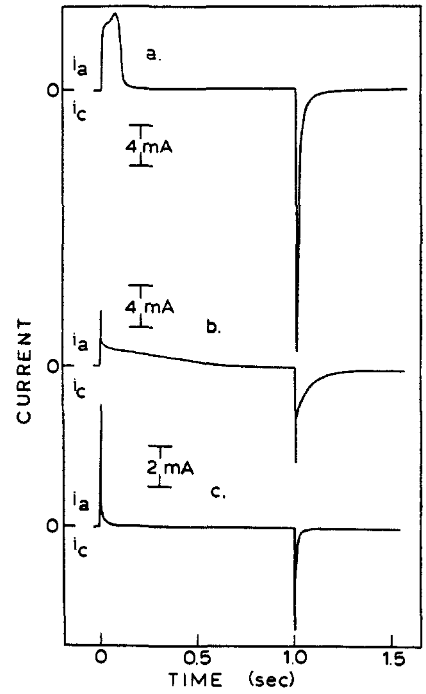

Figure 3. Current transients at 2000-Å MgPc electrodes for the first cycle of a series of potential steps from 0.0–0.9 and back to 0.0 V in (a) 1.0 M KCl, (b) 1.0 M $NaClO_4$, and (c) 0.5 M KHP.

The growth of charge capacity in the presence of biphthalate is unique in our experience. It must result from some kind of accommodation of the film to the anions available in the system. One possibility is a physical rearrangement that gives biphthalate greater access to phthalocyanine sites, perhaps via grain boundaries and defects. On the other hand, it may be physically difficult to achieve such a rearrangement in a manner that would leave the film with enough electron conductivity to show such facile oxidation and rereduction (see below). Perhaps special adsorption effects, like those reported for phthalate on hydroxy aluminum phthalocyanine,[12] play a role in maintaining conductivity. However AlPcOH is quite a different species than MgPc, and we have not been able to observe any alteration of MgPc's UV–vis absorption spectrum or its Raman spectrum after exposure to KHP. [The peak at 1625 cm^{-1} in the Raman spectrum of the immersed unoxidized film (Figure 5) is from biphthalate ion in solution.] An interesting alternative to the explanation involving massive

---

(12) Perrier, G.; Dao, L. H. presented at the 167th Meeting of the Electrochemical Society, Toronto, May 14, 1985; paper 561.

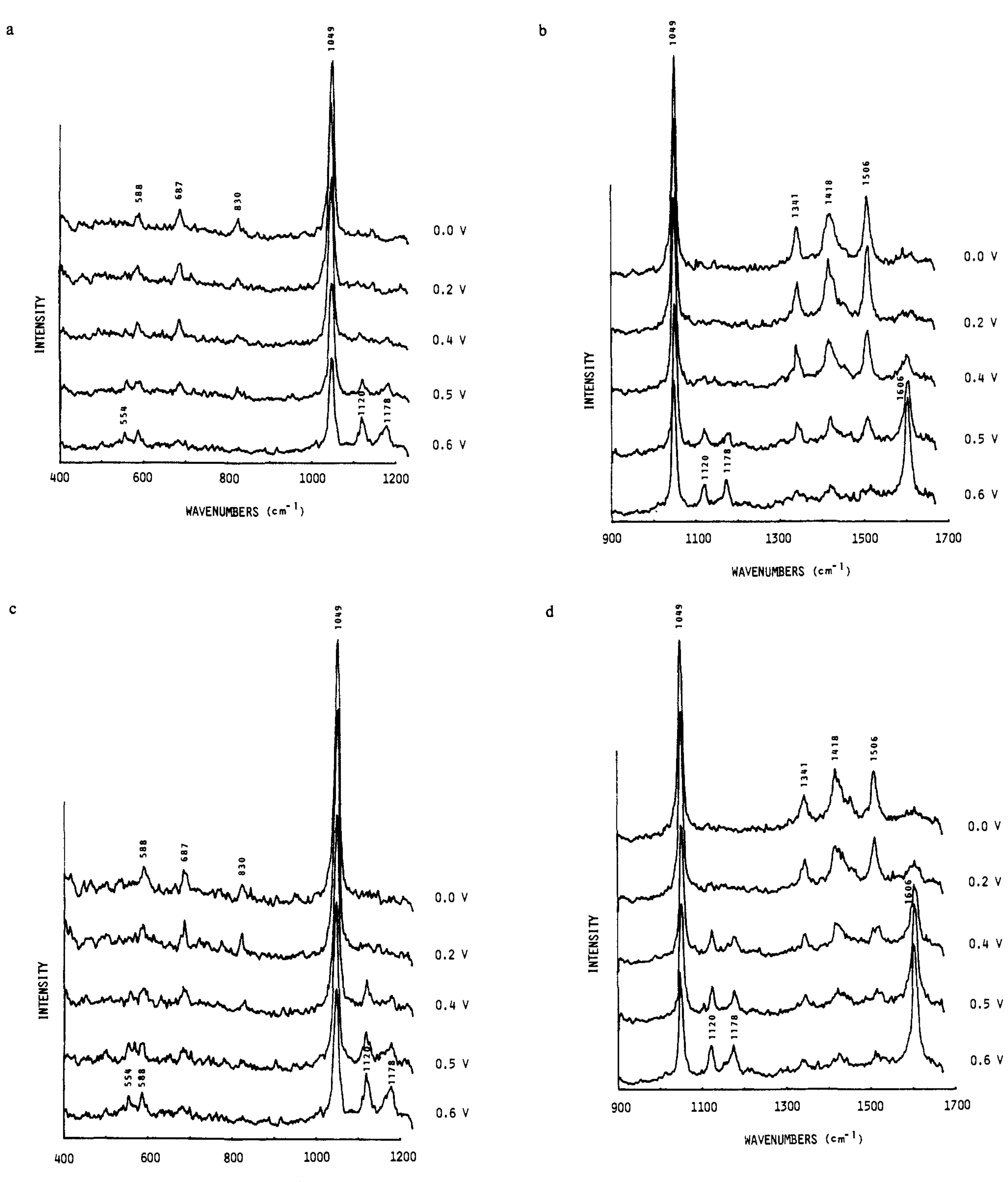

Figure 4. In situ Raman spectra of MgPc electrodes in 1.0 M $NaNO_3$ at 0.0, 0.2, 0.4, 0.5, and 0.6 V vs. SCE for (a) oxidation phase, 400–1200 cm^{-1} range, (b) oxidation phase, 900–1700 cm^{-1} range, (c) rereduction phase, 400–1200 cm^{-1} range, (d) rereduction phase, 900–1700 cm^{-1} range. λ_{exc} = 514.5 nm, maximum 60 mW at sample.

lattice expansion to accommodate HP^- is that charge balance in the film is largely accomplished, in extensively cycled films, by OH^- from water in the system, e.g.,

$$MgPc{\cdot}H_2O \rightarrow MgPc^+OH^- + H^+ + e^- \qquad (3)$$

In this view, a slow hydration of the film would be responsible for the gradual increase in cyclic voltammetric currents.

An attractive feature of this latter model is that it explains the marked difference in peak splittings observed at steady state in the presence of HP^- vs. the other electrolytes. Typically, the separation between anodic and cathodic peak potentials in 1.0 M $NaNO_3$ is about twice the value in 0.4 M KHP. The small ΔE value in KHP suggests that the kinetics of oxidation and rereduction are more facile than in systems with smaller anions. Such behavior would not be expected if anion motion governed the kinetics in all cases, but it is compatible with the existence of the charge compensation scheme expressed in eq 3 for films cycled in KHP, because protons could be expected to move very rapidly into and out of the film. Additional experiments would be needed to confirm or refute this idea.

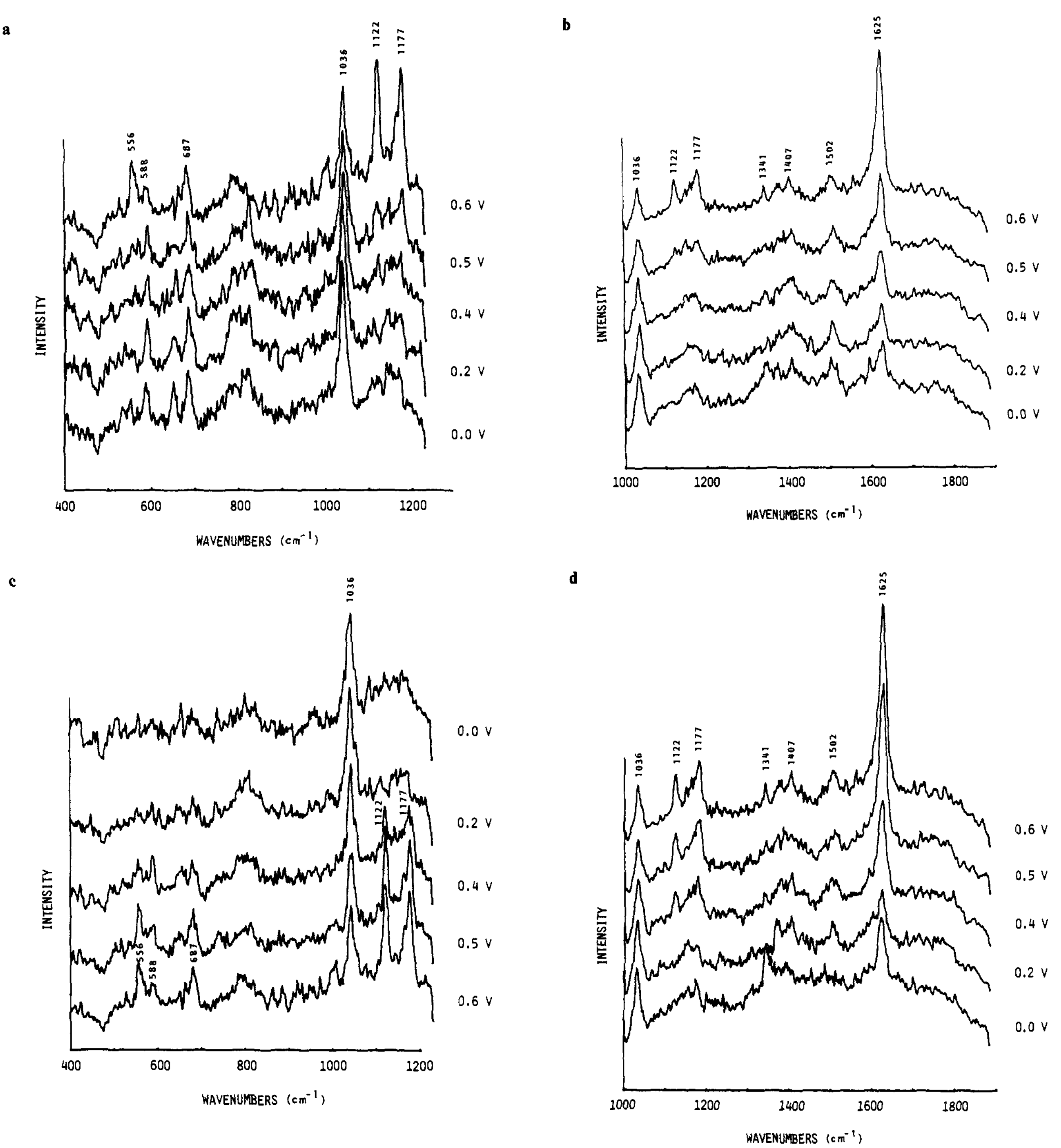

Figure 5. In situ Raman spectra of MgPc electrode in 0.4 M KHP at 0.0, 0.2, 0.4, 0.5, and 0.6 V vs. SCE for (a) oxidation phase, 400–1200 cm^{-1} range, (b) oxidation phase, 1000–1900 cm^{-1} range, (c) rereduction phase, 400–1200 cm^{-1} range, (d) rereduction phase, 1000–1900 cm^{-1} range. λ_{exc} = 514.5 nm, maximum 60 mW at sample.

In Situ Raman Spectra. These supporting electrolytes were also used in a study of the Raman spectra of the films as they were cycled between 0.0 and 0.6 V vs. SCE. Spectra for a 1000-Å film electrode in 1.0 M $NaNO_3$ are shown in Figure 4. Parts a and b of Figure 4 were recorded during the oxidation phase, whereas parts c and d were recorded during rereduction.

Notable was the behavior of the Raman bands at 687, 830, 1341, 1418, and 1506 cm^{-1}. These were intense in the spectrum observed at 0.0 V, but they disappeared almost completely at 0.6 V. Gradual intensity drops for those Raman bands were observed when potential was stepped from 0.4 to 0.5 V, where the oxidation current starts to flow. In situ Raman spectra recorded in the rereduction phase showed that these peaks reappeared, and exactly the same spectra were observed at 0.0 V before and after the oxidation and rereduction cycle.

In contrast to this behavior, the peak intensity at 588 cm^{-1} was unchanged throughout the oxidation and rereduction cycle.

New bands appeared at 554, 1120, 1178, and 1606 cm^{-1} when the potential was set to 0.6 V vs. SCE, but they disappeared when the potential was returned to 0.0 V vs. SCE.

The strong band at 1049 cm^{-1} is due to NO_3^- anions in the aqueous electrolyte. Its intensity decreased almost 50% during the oxidation phase, but the signal returned to the original level when the rereduction phase was completed, as shown in Table II. The intensity drop may be due either to (a) the depletion of NO_3^- in the electrolyte zone situated in the very thin space between the quartz window of the cell and the MgPc thin film electrode or (b) an optical effect caused by altered optical characteristics of the MgPc thin film during the oxidation. The intensity of Raman scattering at 3360 cm^{-1}, observed for the O–H

Table II. Effect of Applied Potential on Raman Scattering from Anions

phase	potential/V vs. SCE	intnsty at 1049 cm^{-1} (1 M $NaNO_3$)/cnts/s	intnsty at 1036 cm^{-1} (0.4 M KHP)/cts/s
	0.0	2111	1048
	0.2	2175	1068
oxidation	0.4	1999	996
	0.5	1395	823
—	0.6	1156	834
	0.5	1426	816
reduction	0.4	1679	904
	0.2	2078	1007
	0.0	2212	1026

stretch of ethanol in an ethanol–water mixture with 0.3 M Et_4NClO_4, also decreased approximately 25% when a thin film NiPc electrode was oxidized at 1.0 V vs. SCE. This result rather supports the view that the redox state of the metal phthalocyanine layer affects the laser power in the gap between the film and the window. Consequently, a much lower level of Raman scattering from both anions and solvent molecules would result in the presence of an oxidized film.

Raman spectra observed in other supporting electrolytes were basically the same as those recorded in 1.0 M $NaNO_3$, except in 0.4 M KHP. Spectra were recorded at several potentials between 0.0 and 0.6 V vs. SCE during the first oxidation and rereduction cycle in 0.4 M KHP solution. The results are shown in Figure 5. Parts a and b of Figure 5 are spectra recorded in the first oxidation phase, and parts c and d are for the first rereduction phase. The Raman peaks at 588, 687, 1407, and 1502 cm^{-1} were basically unchanged during the first oxidation and rereduction cycle. Thus, a major portion of the film was not oxidized in the first positive excursion, as one should expect on the basis of the previously discussed cyclic voltammetric results in KHP. However, new peaks did appear at 556, 1122, 1177 and 1625 cm^{-1} when the electrode potential was stepped to 0.6 V vs. SCE. The frequencies of the first three of these bands are identical with those of the corresponding bands for $NaNO_3$ solution, but the new peak at 1625 cm^{-1} was displaced approximately 20 cm^{-1} from the apparently corresponding peak (1606 cm^{-1}) observed in $NaNO_3$ solution. A peak at 1036 cm^{-1}, which is from aquated HP^- anions, again dropped in intensity, although the drop was only 20%, apparently reflecting the limited oxidation of the MgPc film in KHP.

The symmetry of MgPc is D_{4h} and 55 normal modes are Raman active.[9c,13] The assignments of observed Raman peaks may be classified into several groups. Vibrational frequencies from phthalocyanines in the range 1250–1600 cm^{-1} can be mainly attributed to C=C and C=N stretching in the pyrrole and benzene rings in isoindole moieties.[9a,14] In this range are three major bands at 1341, 1418, and 1506 cm^{-1} in the MgPc spectra. They almost completely disappeared when the film was oxidized. During oxidation of the MgPc film, the new peaks that appeared in $NaNO_3$ and KHP solutions at 1606 and 1625 cm^{-1}, respectively, are also in this frequency range. The results indicate that the pyrrole moieties are strongly affected by oxidation. New bands at 1120 and 1178 cm^{-1} from the oxidized film could be attributed to C–H deformation and H–C–C in-plane bending of the benzene rings, respectively.[13] The gradual appearance and disappearance of these peaks upon oxidation and rereduction indicate the possibility of these modes being Raman inactive while MgPc is in the reduced form with D_{4h} symmetry. The disappearance of bands at both 687 and 830 cm^{-1}, which are due to vibrations of the inner macrocycle, indicates that oxidation distorted this part of the ligand.

The only major peak that was not affected by the oxidation was a band at 588 cm^{-1}, which has been assigned as an isoindole ring deformation.[9a] The 588-cm^{-1} peak seems to be rather interesting. Peaks between 700 and 400 cm^{-1} have been attributed by Stymne et al.[14] to benzene ring vibrations in interaction with the adjacent pyrrole ring. The 588-cm^{-1} peak may be associated with a coupled phthalocyanine ring vibration. Our results show that only this peak is unaffected by applied external potential, even though other vibrations associated with the isoindole rings show drastic changes as a result of possible molecular distortion. The presence of the 588-cm^{-1} peak in the oxidized species, which may not be truly of D_{4h} type, suggests a transformation of the vibration into another Raman active vibrational mode of lower symmetry. The new weak band appearing at 554 cm^{-1} in the oxidized system may be due to a deformation of the phthalocyanine macrocycle involving the bridging nitrogens.

A band observed at 253 cm^{-1} in the Raman spectrum of a MgPc thin film (1000 Å) recorded in air could be assigned as a magnesium–nitrogen vibration. However, higher scattering signals from supporting electrolytes in this spectral range created difficulty in observing the effect of oxidation potential on the 253-cm^{-1} band. Magnesium in a 2+ oxidation state is not expected to be oxidized prior to the ring portions of the molecules, but one would expect some intensity change in the Raman band at 253 cm^{-1}, because the oxidized molecule may be distorted from the planar structure of the reduced form. Our results for nickel phthalocyanine thin film electrodes showed such behavior. Bands at both 247 and 261 cm^{-1} disappeared upon the application of an oxidizing potential (1.1 V vs. SCE) at the electrode. The original intensities were restored when the electrode was rereduced in 1.0 M $NaNO_3$ solution.[15]

The high intensity band at 1625 cm^{-1} in the spectrum of oxidized MgPc in KHP solution shows a clear difference in frequency from the apparently corresponding peaks observed in other supporting electrolytes at 1606 cm^{-1}. As mentioned above, MgPc may have a special interaction with water and hydroxide in KHP solution. The other three anions (NO_3^-, Cl^-, and ClO_4^-) are much weaker Lewis bases, and the degree of distortion imposed on MgPc molecules by those anions may be similar.

Another possible cause for the observed spectral changes is an alteration in packing or crystalline structure by the interaction with anions and water molecules upon oxidation of MgPc film. Upon oxidation, MgPc undergoes a change in color. Initially it is blue when viewed against the gold/glass substrate, but the color changes to a copper (or shiny light brown) color upon oxidation. When the thin film is rereduced, the color changes to green. The color change between light brown and green was reversible when oxidation and rereduction potentials were applied repeatedly. Annealing the rereduced film at 125 °C for 24 h made the film change from green to greenish blue but did not restore the original color. Since our Raman spectroscopic data during oxidation and rereduction process showed complete reversibility, it is apparent that alterations in local structure (within a molecule or involving coordination) are not responsible for imperfect color reversibility in the first oxidation–rereduction cycle. Green and Faulkner[8] interpreted the effect in terms of a lattice distortion affecting the Davydov splitting. Such an interpretation is consistent with the Raman data.

Auger Electron Spectroscopy. Studies of the oxidation and rereduction of MgPc films were carried out for electron spectroscopic examination in both KPF_6 and LiCl. The surface AES spectra for a PF_6^- solution are presented in Figure 6. Curve a is the spectrum for a 2000-Å MgPc film held at 0.0 V for 5 min. Curve B shows the spectrum for a like film held at 0.8 V for 5 min. The depth profiles for this same film appear in Figure 7. Curve b represents the fluorine signal in the unoxidized MgPc film, whereas curve c shows the fluorine signal after the film had been held at 0.8 V for 5 min. The carbon signal has been normalized in all samples to curve a so that the fluorine signals can be compared. The carbon-to-fluorine ratio in the oxidized MgPc

---

(13) Wilson, E. B., Jr.; Decius, J. C.; Cross, P. C. *Molecular Vibrations The Theory of Infrared and Raman Vibrational Spectra*; McGraw-Hill: New York, 1955.

(14) Stymne, B.; Sauvage, F. X.; Wettermark, G. *Spectrochim. Acta Part A* **1979**, *35A*, 1195.

(15) Dwarakanath, K.; Tachikawa, H. in preparation.

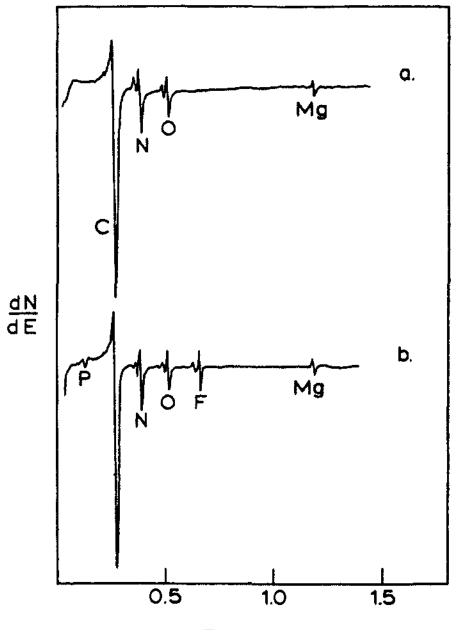

Figure 6. Auger electron spectra: (a) unoxidized MgPc film and (b) MgPc film oxidized at 0.8 V in 0.4 M KPF_6.

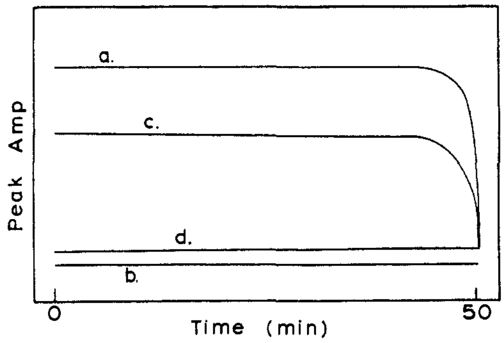

Figure 7. Auger depth profiles for MgPc electrodes treated in 0.4 M KPF_6: (a) carbon peak amplitude for each electrode normalized to this level, (b) fluorine signal for film held at 0.0 V for 5 min (unoxidized sample), (c) fluorine signal after 5 min potential step from 0.0–0.8 V, (d) fluorine signal after 5-min potential steps from 0.0–0.8 and back to 0.0 V.

film suggests that there is only 15% conversion of the film (on the basis of standard AES sensitivities),[16] yet the profile indicates that fluorine is evenly distributed throughout the film. Like HP^-, PF_6^- anions appear to be too large to enter the small, firm crystallites[2a] that make up the MgPc film, but they are apparently small enough to move along grain boundaries and crystal defects into the film. After oxidation and rereduction for 5 min each in PF_6^- solution, MgPc films have a surface AES spectrum that is identical with Figure 6 (curve a). The depth profile of the fluorine signal for this rereduced film (Figure 7, curve d) shows that not all of the PF_6^- has moved out of the film, even after the film is held at the reducing potential for 5 min. Similar results were reported earlier for ZnPc films.[8] Since AES spectra recorded on rereduced MgPc films in NaCl, KCl, RbCl, CsCl, LiCl, $KClO_4$, $NaBF_4$, KPF_6, and $MgCl_2$ solutions gave no signals for any cation, the diffusion of cations into the films was ruled out.

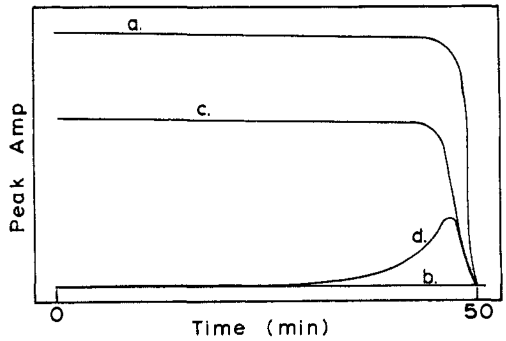

Figure 8. Auger depth profiles for MgPc electrodes treated in 1.0 M LiCl: (a) carbon profile for each electrode normalized to this level, (b) chlorine signal for a fresh electrode that was held at 0.0 V for 5 min in the electrolyte, (c) chlorine signal (× 5) for electrode held at 0.8 V for 5 min, (d) chlorine signal (× 5) after 5-min potential steps from 0.0–0.8 and back to 0.0 V.

Films exercised in Cl^- solutions showed simpler behavior for both the oxidation and rereduction steps. AES depth profiles of MgPc films treated in 1.0 M LiCl solution are presented in Figure 8. The carbon (curve a) to chlorine (curve c) ratio for the oxidized film corresponds roughly to a 100% conversion of the film to $MgPc^+Cl^-$.[15] Curve d indicates that the rereduced MgPc film has lost almost all of the Cl^-, except for a small zone deep in the film next to the gold underlayer. This small zone is consistent with the known tendency for gold to interact strongly with chloride at positive potentials. The nearly complete loss of Cl^- for the rereduced film indicates that the small Cl^- moves freely into and out of the crystallites in the film, as represented by eq 1 and 2.

Acknowledgment. For support of this work, we are grateful to the Department of Energy, Division of Materials Sciences (Contract DE-AC02-76-ER01198, administered by the Materials Research Laboratory of the University of Illinois), the Office of Naval Research (Grant N00014-81-K-0639), and the National Institutes of Health (Grant RR08047).

Registry No. MgPc, 1661-03-6; $MgPc^+$, 53029-46-7; $MgPc^+Cl^-$, 88769-75-9; $NaNO_3$, 7631-99-4; KHP, 877-24-7; KCl, 7447-40-7; $NaClO_4$, 7601-89-0; KPF_6, 17084-13-8; LiCl, 7447-41-8; Au, 7440-57-5.

---

[16] Palmberg, P. W.; Riach, G. E.; Weber, R. E.; MacDonald, N. C. *Handbook of Auger Electron Spectroscopy*; Physical Electronics Industries: Edian, MN, 1972.